Methyl-Group Move in Low-Temperature Rare-Gas Matrixes and Conformational Analysis of 1,4-Dimethoxybenzene

Nobuyuki Akai, Satoshi Kudoh, and Munetaka Nakata*

Graduate School of BASE (Bio-Applications and Systems Engineering), Tokyo University of Agriculture and Technology, Naka-cho, Koganei, Tokyo 184-8588, Japan

Received: June 28, 2002; In Final Form: January 24, 2003

Conformational changes of 1,4-dimethoxybenzene in low-temperature rare-gas matrixes have been investigated by FTIR spectroscopy with an aid of the density-functional-theory calculation. Two stable conformers, *cis*-planar and *trans*-planar, are found to exist in argon matrixes by comparing the observed spectrum with the calculated spectral patterns. The enthalpy difference between the conformers is estimated from the dependence in the population ratio on the nozzle temperature to be 1.12 ± 0.09 kJ mol^{-1}, where cis is more stable than trans. On the other hand, cis changes to trans in krypton and xenon matrixes in dark, in contrast to the stability in the argon matrix. The conversion rate constants are estimated from the decay behavior of a cis band at various matrix temperatures. Dependence of the rate constants on the matrix temperature is found to be inconsistent with the Arrhenius law. The conformational changes in krypton and xenon matrixes are ascribed to the torsional potential changes caused by an interaction between the sample and matrix atoms, where trans is assumed to be stabilized in the order of Ar < Kr < Xe.

Introduction

Quantum tunneling effects play an important role in low-temperature chemistry, where certain reactions which deviate from thermal-equilibrium behavior are characterized by a tunneling probability. The low-temperature matrix-isolation technique has been applied to hydrogen-atom tunneling on a symmetrical potential surface; for example, tropolone,[1−3] malonaldehyde,[4] and 9-hydroxyphenalenone.[5−8] Heavy-atom tunneling has also been observed in matrixes. For example, tautomerism of cyclobutadiene,[9,10] oxygen-atom transfers in NO and O_3 complex,[11] interconversion of ClNO,[12] and rotation of 3-fluoropropene[13] were ascribed to the tunneling effect.

We have focused our attention to the tunneling on an asymmetric potential surface.[14,15] In a recent paper,[14] we reported that the isomerization of hydroquinone occurs in dark at low-temperature and the cis/trans population ratio changes in equilibrium at various matrix temperatures despite a high torsional barrier, 10.8 kJ mol^{-1}. Since no tunneling effect of hydroquinone was observed in the gas phase,[16] we attributed the observed cis−trans equilibrium to a matrix-induced tunneling effect, where its asymmetrical potential surface was expected to be quasi-symmetrical as a result of an interaction between hydroquinone and matrix atoms.

In the present study, we examine the tunneling effect of 1,4-dimethoxybenzene by low-temperature matrix-isolation FTIR spectroscopy with an aid of the density-functional-theory (DFT) method and compare the result with that of hydroquinone. This molecule has five possible conformers by combination of planar or perpendicular with cis or trans, as shown in Figure 1. The torsional barriers of the methyl group around the C−O bond were estimated to be about 0.8 kJ mol^{-1} for all the conformers by ab initio STO-3G calculation.[17] This value is unreliable because its calculation level is too low. The geometrical structures and the relative energies of the conformers were also discussed experimentally and theoretically.[18−22] Some researchers suggested that not only two planar conformers but also two perpendicular ones, cis (C_{2v}) and trans (C_{2h}), exist in the S_0 state, while two stable conformers in the S_1 state are planar but not perpendicular.[20] Tzeng et al. performed the quantum chemical calculation for the S_0 state at the Hartree−Fock level with the 6-31G* basis set, where the methyl group is assumed as a point.[21] They tried to compare their calculated wavenumbers with infrared and Raman spectral data observed in the liquid and solid phases.[23] However, conformational identification was impossible since the bands of all conformers are similar and indistinguishable. They tentatively assigned the vibrational bands to the conformers shown in Figure 1 all together. Thus, one of the present purposes is to measure sharp matrix infrared bands and determine the stable conformations of 1,4-dimethoxybenzene by a vibrational analysis.

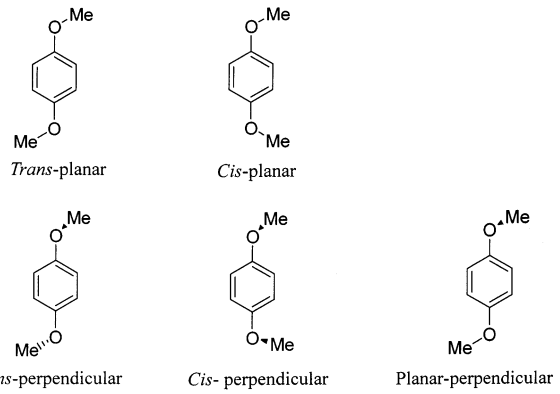

Figure 1. Five possible conformers of 1,4-dimethoxybenzene: Our DFT calculation resulted in that planar isomers are stable but perpendicular ones are unstable.

We have performed the DFT/B3LYP calculation with the 6-31++G** basis set to estimate the energy difference between

* Corresponding author. Tel: +81-42-388-7349. Fax: +81-42-388-7349. E-mail: necom@cc.tuat.ac.jp.

10.1021/jp0215318 CCC: $25.00
Published on Web 03/15/2003

the conformers and the barrier height of rotational isomerization, where the methyl groups are optimized without a point approximation. The obtained spectral patterns are compared with the observed matrix-isolated infrared spectra. Three kinds of rare-gas atoms, Ar, Kr, and Xe, are used to study the influence of matrix medium on the isomerization between the conformers.

Experimental and Calculation Methods

The sample of 1,4-dimethoxybenzene was purchased form Tokyo Chemical Industry Co. Ltd. and used after vacuum distillation. The sample gas was diluted with argon (Nippon Sanso, 99.9999% purity), krypton (Nippon Sanso, 99.999%), or xenon (Tokyo Gas Chemical, 99.999%) in a glass cylinder. The mixing ratio of sample/rare gas was about 1/1500. The premixed gases were expanded through a stainless steel pipe, 1/8- or 1/16-in. diameter equipped with a heating system. The nozzle temperature was monitored by a Chromel−Alumel thermocouple and controlled by a thermostabilizer (CHINO, GK100) using a PID (Proportional plus Integral plus Derivative) action method with a solid-state relay, where the uncertainty of the temperature was within 1 K. The premixed gases passed through the nozzle were deposited in a vacuum chamber on a CsI plate (3 mm × 13ϕ), cooled by a closed-cycle helium refrigeration (CTI Cryogenics, model M-22) at 16 K for argon, 20 K for krypton, and between 18 and 40 K for xenon. The CsI plate was surrounded with an alumilite (γ-Al_2O_3·H_2O) shield pipe (2 mm × 56 ϕ) cooled at 70 K to avoid thermal radiation from windows and walls of the vacuum chamber, except for the path of the infrared beam of the spectrophotometer. A film heater (30 W) to warm the matrix sample was attached at 5 cm distance from the CsI plate. The matrix temperature was monitored continuously by an Au−Chromel thermocouple at a side of the CsI plate and controlled by a thermostabilizer (IWATANI, TCU-4) using a PID action method, where the uncertainty of the temperature was within 0.15 K.

UV radiation from a superhigh-pressure mercury lamp was used to induce photoreaction through a water filter to remove thermal reactions. Infrared spectra of the matrix samples were measured with an FTIR spectrophotometer (JEOL, Model JIR-7000). The spectral resolution was 0.5 cm^{-1}, and the number of accumulation was 64. Other experimental details were reported elsewhere.[24,25]

DFT calculations were performed by using the GAUSSIAN 98 program[26] with the 6-31++G** basis set. The hybrid density functional,[27] in combination with the Lee−Yang−Parr correlation functional (B3LYP),[28] was used to optimize the geometrical structures.

Results and Discussion

Structures of Stable Conformers in an Argon Matrix. Figure 2a shows an infrared spectrum of 1,4-dimethoxybenzene measured in an argon matrix at 16 K. Geometry optimization of 1,4-dimethoxybenzene by the DFT/B3LYP/6-31++G** calculations results in that cis-planar and trans-planar conformers are stable, but perpendicular ones are unstable. So we omit "-planar" in the cis and trans conformers hereafter. The calculated spectral patterns for trans and cis are also shown in Figures 2b and 2c, where a scaling factor of 0.98 is used.[29] By a comparison between the observed and calculated spectra, all the observed bands are assignable to the cis and trans conformers, except for the bands marked with † assigned to a small amount of impurity water. The weak bands marked with * are due to the combination modes of trans as described later.

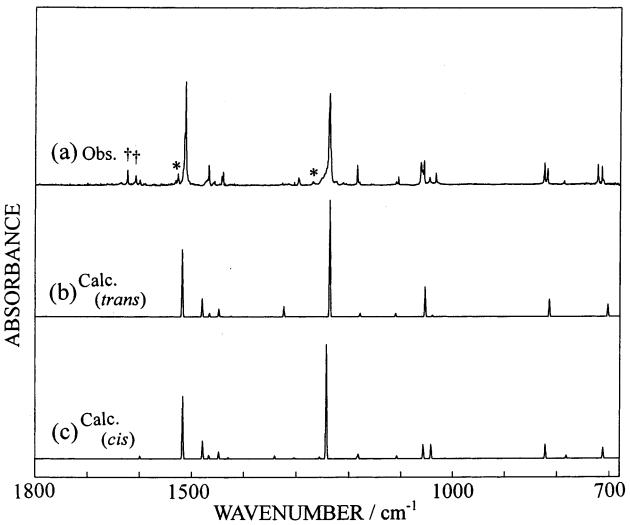

Figure 2. Infrared spectra of 1,4-dimethoxybenzene in an argon matrix at 16 K: (a) Observed matrix spectrum. Bands marked with † represent a small amount of impurity H_2O. Bands marked with * represent combination modes of trans; (b) and (c) Calculated spectral patterns for trans and cis, respectively, obtained by the DFT/B3LYP/6-31++G** calculation, where a scaling factor of 0.98 is used.

The calculated spectral pattern of cis is similar to that of trans. To distinguish the cis and trans bands, we heated the matrix sample from 16 to 28 K and kept it for a long time in dark. In the case of hydroquinone,[14] the population ratio of trans and cis depended on the matrix temperature because isomerization due to hydrogen tunneling occurred according to the Boltzmann distribution law, where the observed spectral change was used to distinguish the infrared bands of trans and cis. However, no spectral changes for 1,4-dimethoxybenzene was observed, unlike hydroquinone. Then we irradiated the matrix sample by UV light from a superhigh-pressure mercury lamp. No spectral change was observed when an optical filter UV-32 ($\lambda \geq 310$ nm) was used. When the filter was removed, however, photodissociation of cis and trans occurred unlike photoisomerization seen in several molecules isolated in rare-gas matrixes.[30−35] We tried to assign the infrared bands of photoproducts but found that they were inconsistent with the spectral patterns of benzoquinone produced by dissociation of two methyl groups or possible other intermediates optimized by the DFT method. Fortunately, it is noted that the intensities of the trans bands become weaker than those of cis by the irradiation, as shown in Figures 3a and 3b measured before and after 15-min UV irradiation, respectively. Since the photodissociation rate of trans is faster than that of cis, the trans bands can be distinguished from the cis bands by the spectral change; the bands appearing at 825, 787, and 723 cm^{-1} are assigned to cis, while those appearing at 819 and 715 cm^{-1} are trans. Our assignments for the bands observed in the whole spectral region are summarized in Table 1 with the corresponding calculated wavenumbers and their relative intensities.

Enthalpy Difference between Cis and Trans in an Argon Matrix. Our DFT calculations result in that cis is more stable than trans by 0.63 kJ mol^{-1}. This finding is opposite to that in hydroquinone where trans is more stable than cis by 0.56 kJ mol^{-1}.[14] To determine which conformer of 1,4-dimethoxybenzene is stable and to estimate the energy difference between the conformers experimentally, we have examined the dependence in the cis/trans population ratio on the deposition nozzle temperature. It is well-known that matrix-isolated samples keep the population ratio in the gas phase at the deposition

TABLE 1: Observed and Calculated Vibrational Wavenumbers (in cm^{-1}) and Relative Intensities of 1,4-Dimethoxybenzene in an Argon Matrix at 16 K

cis-planar				trans-planar				
obs		calc		obs		calc		
$\tilde{\nu}$	int	$\tilde{\nu}^a$	int	$\tilde{\nu}$	int	$\tilde{\nu}^a$	int	sym
3048	0.7	3161	1.2			3160	0	a_g
		3151	1.1	3030	3.8	3159	2.9	b_u
3017	7.3	3147	2.1			3140	0	a_g
2942	2.1	3137	1.4	2922	1.9	3138	2.8	b_u
		3084	0.4			3084	0	a_g
2903	0.5	3084	9.1	2917	1.9	3084	9.2	b_u
2894	1.2	3008	18.0	2898	1.7	3009	17.3	b_u
		3008	0.0			3009	0	b_g
2841	1.5	2950	14.4			2950	0	a_g
2839	8.7	2949	10.7	2850	3.2	2950	25.9	b_u
		1633	0.3			1635	0	a_g
1600	11.3	1599	2.6			1597	0	a_g
1512	100	1517	54.9	1515	56.9	1519	56.0	b_u
		1482	0.2			1480	0	a_g
(1468	23.1)[b]	1479	15.9	(1468	23.1)[b]	1480	15.9	b_u
(1460	5.0)[b]	1467	3.1			1467	0	b_g
		1466	0.0	(1460	5.0)[b]	1467	2.9	a_u
		1453	0.1			1453	0	a_g
1440	15.6	1448	6.3	1443	10.9	1450	6.3	b_u
		1430	1.2			1426	0.7	b_u
1338	2.9	1341	2.8	1297	9.4	1324	8.1	b_u
1305	3.9	1304	0.9			1307	0	a_g
1248	11.7	1256	1.5			1278	0	a_g
1239	96.6	1243	100	1238	100	1239	100	b_u
		1184	1.5			1183	0	a_g
1185	23.2	1182	4.2	1182	3.8	1181	3.3	b_u
		1170	0.2			1168	0	a_g
		1149	0.3			1148	0	b_g
		1149	0.0			1148	0.3	a_u
1106	10.2	1108	2.4	1111	3.3	1113	2.8	b_u
1057	29.9	1057	12.5	1063	23.3	1056	26.0	b_u
1046	6.5	1042	12.7			1044	0	a_g
		999	0.0			999	0.0	b_u
		938	0.0			928	0.1	a_u
		883	0.0			905	0	b_g
		823	0.3			823	0	a_g
825	29.3	822	12.3	819	18.0	816	14.6	a_u
787	3.3	782	2.8			792	0	b_g
723	21.2	712	9.7	715	19.5	703	10.3	b_u
		678	0.0			680	0	b_g
		634	0.0			639	0	a_g

[a] A scaling factor of 0.98 is used. [b] Cis and trans bands overlap with each other.

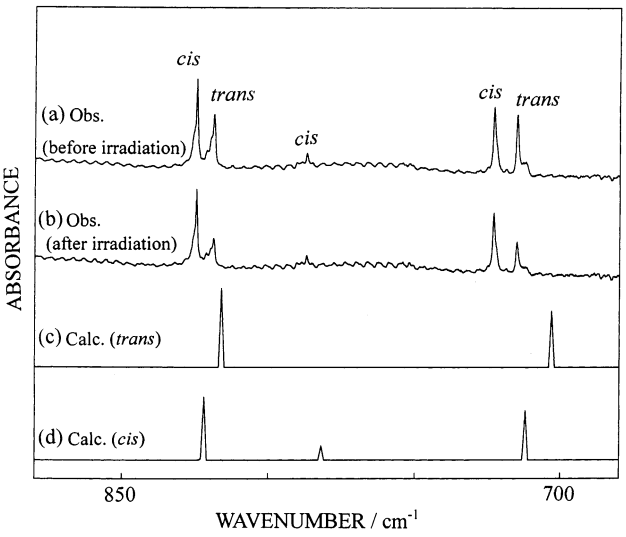

Figure 3. Expanded infrared spectra of 1,4-dimethoxybenzene in an argon matrix at 16 K: (a) and (b) Observed spectra measured before and after 15-min UV irradiation, respectively; (c) and (d) Calculated spectral patterns for trans and cis, respectively, obtained by the DFT/B3LYP/6-31++G** calculation, where a scaling factor of 0.98 is used. Trans decreases more rapidly than cis by the irradiation.

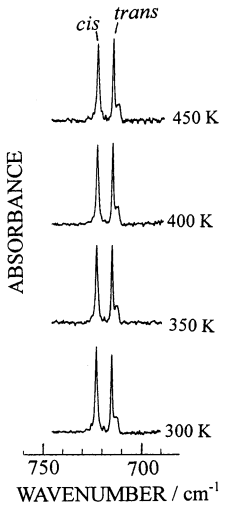

Figure 4. Spectral changes of 1,4-dimethoxybenzene in argon matrixes at various nozzle temperatures.

temperature;[36−39] for example, we reported that the enthalpy difference of 1,2-dichloroethane obtained by the same experimental system was consistent with the value estimated by other experimental methods.[37] As shown in Figure 4, the intensity of the cis band (723 cm^{-1}) decreases as the nozzle temperature increases, while the trans band (715 cm^{-1}) increases. The logarithm of the absorbance ratio between the 715 and 723 cm^{-1} bands versus the inverse of the nozzle temperature is plotted in Figure 5. The enthalpy difference between the conformers is estimated from the slope by a least-squares fitting to be 1.12 ± 0.09 kJ mol^{-1}. The fact that cis is more stable than trans is consistent with the result of the DFT calculation, where the enthalpy difference is estimated to be 0.75 kJ mol^{-1} from the energy difference, 0.63 kJ mol^{-1}, by the enthalpy correction. The difference between the observed and calculated values may be caused by an interaction between 1,4-dimethoxybenzene and argon atoms, as described later.

Isomerization from Cis to Trans in Xenon and Krypton Matrixes. In a spectrum measured immediately after deposition with xenon atoms on a CsI plate cooled at 30 K, the intensities of the cis bands are found to be weaker than those of trans, as shown in Figure 6a. The observed bands are slightly shifted to the lower-wavenumber side from those observed in the argon matrix; for example, the cis bands appearing at 825 and 723 cm^{-1} are shifted to 821 and 718 cm^{-1}, respectively, while the trans bands appearing at 819 and 715 cm^{-1} are shifted to 817 and 710 cm^{-1}, respectively. The cis band appearing at 787 cm^{-1} is unchanged within 1 cm^{-1}.

When the matrix sample was kept in dark, a spectral change due to the cis−trans isomerization was observed. A difference spectrum between those measured immediately after deposition and after 30 min keeping the matrix in dark is drawn in Figure 7 with a corresponding spectral pattern obtained by the DFT/B3LYP/6-31++G** calculation. The calculated spectral pattern, where trans is up and cis is down, reproduces the observed difference spectrum satisfactorily, except for the positive bands appearing at 1522, 1507, and 1262 cm^{-1} and the negative doublet bands at 1246 and 1236 cm^{-1} in the observed difference spectrum. The former bands may be assigned to combination modes and the latter bands to Fermi resonance with the intense

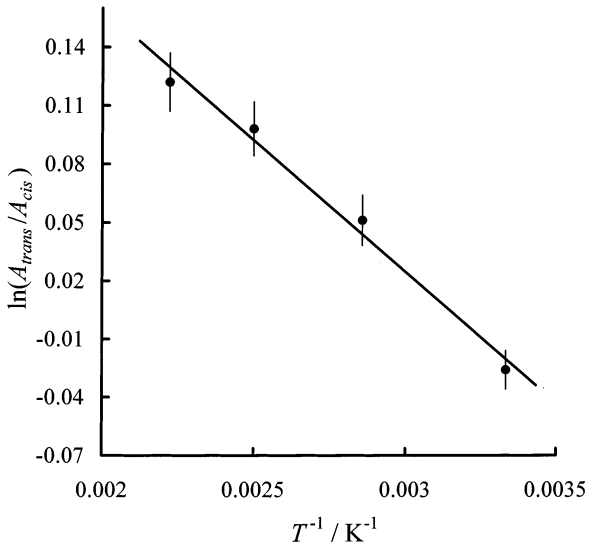

Figure 5. Logarithmic plot of absorbance ratio versus inverse of nozzle temperature: A_{cis} and A_{trans} represent the absorbances of cis (723 cm^{-1} band) and trans (715 cm^{-1} band), respectively. Solid line represents the calculated values obtained by a least-squares fitting. Error bars represent uncertainties in peak area measurements.

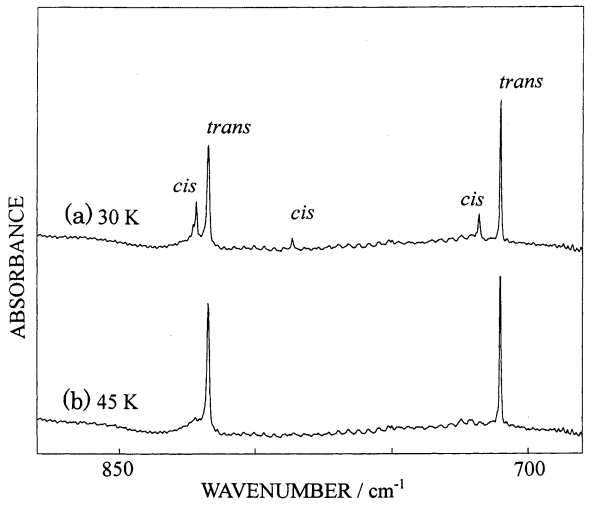

Figure 6. Infrared spectra of 1,4-dimethoxybenzene in a xenon matrix: (a) and (b) Measured at 30 and 45 K, respectively.

1243 cm^{-1} band. We conclude that the more stable conformer, cis, changes to the less stable conformer, trans, in dark. A similar phenomenon was observed in ethanediamine; the more stable conformer, gauche, changes to the less stable conformer, trans, in rare-gas matrixes in dark.[33]

When the matrix sample was heated to 45 K, the cis bands disappeared completely and the intensities of the trans bands increased as shown in Figure 6b. On the other hand, no cis bands appeared by decreasing the matrix temperature, in contrast to the result of hydroquinone, where the cis−trans isomerization occurred reversibly at low temperature through tunneling.[14] The reason the more stable cis conformer of 1,4-dimethoxybenzene changes to the less stable trans conformer is discussed later.

Rotational isomerization from cis to trans in krypton matrixes has also been examined. The cis bands appearing at 825, 787, and 723 cm^{-1} in argon matrixes were observed at 824, 787, and 721 cm^{-1} in krypton matrixes at 40 K, while the trans bands appearing at 819 and 715 cm^{-1} in argon matrixes were observed at 818 and 713 cm^{-1}. The wavenumbers of these bands are between those measured in argon and xenon matrixes. The cis/trans relative intensity is smaller than that in the argon matrix. The intensities of the cis bands slightly decreased and those of trans increased when the matrix sample was kept in dark for 240 min. The cis bands remained in krypton matrixes even if the temperature was heated to 50 K in contract to the result obtained in xenon matrixes.

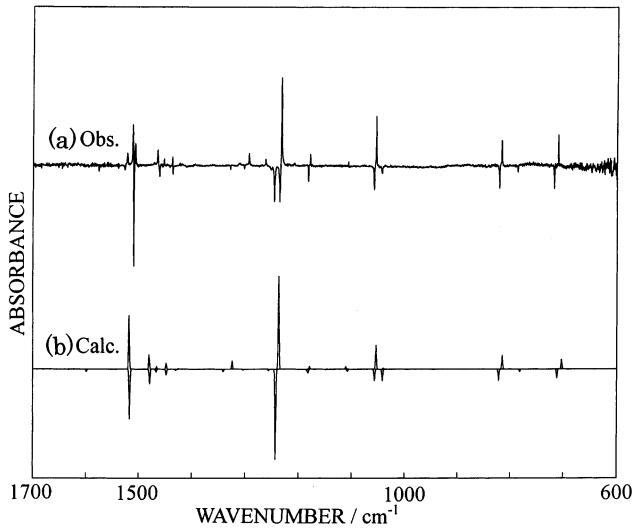

Figure 7. Spectral change in a xenon matrix in dark: (a) Observed difference spectrum between those measured immediately after deposition and after 30-min holding at 30 K; (b) Calculated difference spectrum. Trans is up and cis is down.

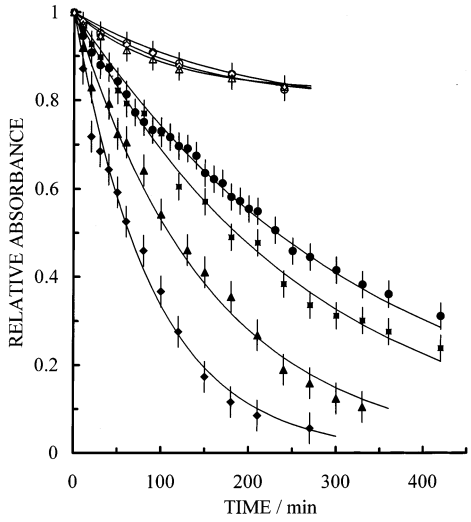

Figure 8. Decay behavior of the cis band (718 cm^{-1}) in krypton and xenon matrixes in dark: Closed circles, squares, triangles, and diamonds represent measurements at 18, 20, 25, and 30 K in xenon matrixes, respectively. Open squares, triangles, and diamonds represent measurements at 20, 30, and 40 K in krypton matrixes, respectively. Error bars represent uncertainties in peak area measurements. Solid curves represent the calculated values obtained by a least-squares fitting.

Conversion Rate. Behavior of the cis−trans isomerization in krypton and xenon matrixes depends on time, matrix temperature, and matrix medium. The rate constant of isomerization is estimated by a plot of the relative absorbance decay of the cis band (718 cm^{-1}) in Figure 8, where the absorbance is normalized by one observed in the first spectral measurement after deposition. The error bars represent uncertainties in peak area measurements. As described before, the intensities of the cis band in xenon matrixes decrease rapidly as the matrix temperature increases. On the other hand, the decay behavior

TABLE 2: Dependence of Conversion Rate Constants, *k*, from Cis to Trans on Matrix Temperature, *T*, and Matrix Medium

T/K	*k*/min^{-1}
in xenon	
18	0.0030 ± 0.0002[a]
20	0.0037 ± 0.0002
25	0.0064 ± 0.0006
30	0.0109 ± 0.0011
40	n.d.[b]
in krypton	
20	0.005 ± 0.004
30	0.008 ± 0.004
40	0.010 ± 0.003

[a] Three times standard deviation. [b] The conversion at 40 K is too rapid for observation of the cis band.

in krypton matrixes is similar in the temperature range between 20 and 40 K.

We assume that the isomerization from cis to trans can be described by a first-order rate equation,

$$-\mathrm{d}A_{\mathrm{cis}}/\mathrm{d}At = kA_{\mathrm{cis}} \quad (1)$$

$$A_{\mathrm{cis}} = A_{\mathrm{cis},t=0} \exp(-kt) \quad (2)$$

where A_{cis} and k represent the absorbance of the cis band and the rate constant at the matrix temperature, T, respectively. In consideration of normalization, eq 2 is modified as

$$A_{\mathrm{cis}}/A_{\mathrm{cis},t=0} = \exp(-kt) \quad (3)$$

Then, the isomerization rates in xenon matrixes are estimated from the decay behavior by a least-squares fitting. A small discrepancy between the experimental and calculated values may be caused by the baseline oscillations in the observed spectra.

On the other hand, the absorbance of the cis band in krypton matrixes does not approach zero at infinite time. This fact suggests that the population distribution of cis and trans becomes in equilibrium as discussed later. We assume the following equation instead of eq 2:

$$A_{\mathrm{cis}} = (A_{\mathrm{cis},t=0} - A_{\mathrm{cis},t=\infty}) \exp(-kt) + A_{\mathrm{cis},t=\infty}. \quad (4)$$

In consideration of normalization, eq 4 is modified as

$$A_{\mathrm{cis}}/A_{\mathrm{cis},t=0} = (1 - A_{\mathrm{cis},t=\infty}/A_{\mathrm{cis},t=0}) \exp(-kt) + A_{\mathrm{cis},t=\infty}/A_{\mathrm{cis},t=0} \quad (5)$$

The values of $A_{\mathrm{cis},t=\infty}/A_{\mathrm{cis},t=0}$ obtained by a least-squares fitting are 0.77 ± 0.03, 0.80 ± 0.02, and 0.82 ± 0.01 at the matrix temperatures of 20, 30, and 40 K, respectively. This means that about 20% conversion from cis to trans occurs after the first spectral measurement. The isomerization rates for xenon and krypton matrixes obtained are summarized in Table 2.

Figure 9 shows a plot of the *k* values for xenon matrix against the inverse of the matrix temperature, where the error bars represent three times standard deviation calculated by the least-squares fitting. We assume that the behavior of *k* between 18 and 30 K is linear and derive the effective activation energy, E_{act}, and the frequency factor, A, by using the Arrhenius equation:

$$k = A \exp(-E_{\mathrm{act}}/RT) \quad (6)$$

The calculated values for E_{act} and A are 0.48 ± 0.13 kJ mol^{-1} and 0.070 ± 0.021 min^{-1}, respectively, where the uncertainties

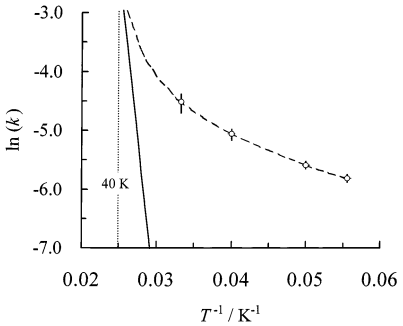

Figure 9. Plot of the conversion rate constant against the inverse of xenon-matrix temperature: Dotted line at 40 K represents asymptotic line (we could not observe the spectrum of cis at the matrix temperature of 40 K because the isomerization rate constant is too large). Solid line represents the calculated slope of the Arrhenius plot when the activation energy is assumed to be 9.27 kJ mol^{-1} obtained by the DFT calculation.

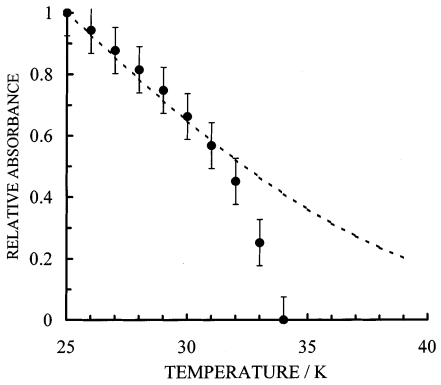

Figure 10. Decay behavior of the cis band (718 cm^{-1}) when the xenon matrix temperature was increased continuously with a rate of 1 K/10 min: The broken curve represents the calculated values obtained using eq 6 with assumption of the Arrhenius law.

represent three times standard deviations. This activation energy should correspond to the barrier height of isomerization measured from the energy minimum of cis. However, the obtained value is much smaller than the estimate from the DFT calculation, 9.27 kJ mol^{-1}, and is curiously almost a half of the enthalpy difference between the two conformers, 1.12 kJ mol^{-1}.

The *k* value at 40 K is calculated to be 0.016 ± 0.007 min^{-1} using the obtained activation energy and frequency factor. If this were true, we could have observed the decay of the cis band at this temperature. However, it was impossible since the conversion from cis to trans occurred too rapidly. This finding strongly suggests that the isomerization behavior cannot be explained by a single Arrhenius plot.

The inflection temperature was determined by measuring the infrared spectra at 10 min interval with increasing matrix temperature continuously with a rate of 1 K/10 min. The decay behavior of the cis band at 718 cm^{-1} is drawn in Figure 10, where a decay curve denoted as a broken line represents the calculated values obtained using eq 6 and assuming the activation energy of 0.48 kJ mol^{-1} and the frequency factor of 0.016 min^{-1}. The intensity of the cis band starts to decrease abruptly at 32 K.

The uncertainties of the *k* values for krypton matrix are large because the isomerization change is small, in contrast to the results of xenon matrix. We could not precisely determine the effective activation energy for krypton matrix.

Possible Rotational Isomerization Mechanism. There are many reports on rotational isomerization in rare-gas matrixes induced by UV, visible-light irradiation, infrared ray from IR

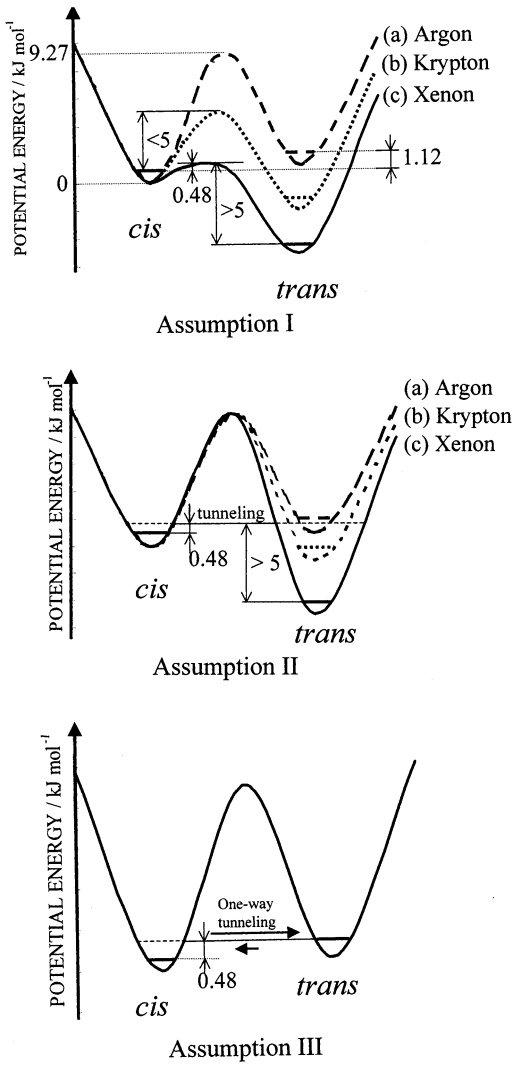

Figure 11. Assumptions for schematic potential curves for 1,4-dimethoxybenzene: Assumption I: Isomerization due to thermal equilibrium process. Torsional barrier height and energy minimum in the potential surfaces decrease in order of Ar > Kr > Xe by the matrix effects. Assumption II: Isomerization due to tunneling effect. Torsional barrier height is unchanged in the rare-gas matrixes, while energy minimum decreases in order of Ar > Kr > Xe. Assumption III: Isomerization due to one-way tunneling. Potential surfaces are unchanged in the rare-gas matrixes. Tunneling probability increases in the order of Ar < Kr < Xe.

spectrophotometer, thermal equilibrium, and tunneling effect.[30−35] One possibility for the isomerization of 1,4-dimethoxybenzene is an infrared-induced methyl-group move. However, this possibility can be ruled out because the isomerization occurs in dark as well as in infrared radiation of spectrophotometer. We discuss other possibilities as follows.

Conversion in Thermal Equilibrium. This process occurs in low-temperature matrixes when the potential barrier is lower than about 5 kJ mol^{-1}.[40] Since the calculated barrier height of 1,4-dimethoxybenzene is 9.27 kJ mol^{-1}, the isomerization does not seem to occur in argon matrixes. This is supported by the observation of the population change of cis/trans at various nozzle temperatures, from which the enthalpy difference was determined to be 1.12 ± 0.09 kJ mol^{-1}. The potential energy curve of 1,4-dimethoxybenzene in argon matrixes is schematically drawn in Assumption I-(a) in Figure 11. If the barrier height is reduced below 5 kJ mol^{-1} by interaction with krypton atoms, as shown in Assumption I-(b), and trans is slightly stabilized more than cis, the isomerization from cis to trans may occur in krypton matrixes and the population ratio may reach an equilibrium. This potential surface can explain the fact that the cis bands in krypton matrixes remain at infinite time.

Similarly, complete disappearance of the cis bands in xenon matrixes by an irreversible reaction may be explained by assuming that trans is more stable than cis by at least 5 kJ mol^{-1}. The potential energy surface of 1,4-dimethoxybenzene in xenon matrixes is schematically drawn in Assumption I-(c) in Figure 11, where the potential barrier is assumed to be equal to the effective activation energy, 0.48 kJ mol^{-1}, estimated from the dependence of the rate constants on the matrix temperature. However, one may wonder whether such a large matrix effect for 1,4-dimethoxybenzene is possible despite the small structural difference between cis and trans.

There are two kinds of matrix effects for this phenomenon: interaction force field and physical matrix size. The former originates from van der Waals and quadrapole interactions between 1,4-dimethoxybenzene and rare-gas atoms. As the number of electrons in rare-gas atoms increases, the interaction increases and the energy of guest molecules is more stabilized.[31] However, not trans but cis is stabilized by this matrix effect in the order of Ar < Kr < Xe. This result is opposite to our observation. On the other hand, the latter matrix effect is explained by the diameter of rare-gas matrixes: 376, 400, and 432 pm for Ar, Kr, and Xe, respectively.[41] The diameter of the methyl group is 418 pm, which is larger than Ar and smaller than Xe. Then, the free space for methyl-group move increases and the torsional barrier decrease with the size of rare-gas atom. In fact, the 723 (cis) and 715 cm^{-1} (trans) bands observed in the argon matrixes are shifted to the lower-wavenumber side, 721 and 713 cm^{-1} in krypton and 718 and 710 cm^{-1} in xenon matrixes. These observations imply that the potential surface is influenced by the matrix medium. If the free space made of rare gases is symmetrical and fit for the structure of trans more than cis, the energy of trans is stabilized relatively. This speculation can explain the potential changes drawn in Figure 11. The fact that the obtained conversion rate constant (k) does not follow the single Arrhenius plot may be explained by the dependence of the free space on the matrix temperature.

Tunneling Effect. Another possibility is the matrix-induced methyl-group tunneling shown in Assumption II in Figure 11, where the torsional barrier height is assumed to be nearly equal in Ar, Kr, and Xe matrixes. If the obtained effective activation energy of 1,4-dimethoxybenzene in xenon matrixes, 0.48 kJ mol^{-1}, corresponds to the energy level for tunneling by a perturbation of matrix medium as in the case of hydroquinone,[14] the isomerization from cis to trans can be explained by methyl-group tunneling through an energy level with 0.48 kJ mol^{-1}. However, methyl group seems to be too heavy for a tunneling particle, although heavy-atom tunneling is proposed for cyclobutadiene[9,10] and NO−O_3 system ,[11] ClNO,[12] and 3-fluoropropane[13] in matrixes, as described in the Introduction. Other direct evidences or other examples to show the methyl-group tunneling are required.

Besides the matrix effect for the potential surface, it is also possible to explain the inconsistency between our observation and the Arrhenius law. In this case, however, one must assume one-way tunneling to explain the irreversible isomerization; the tunneling probability from trans to cis in xenon matrixes is negligible in comparison with that from cis to trans (drawn in Assumption III in Figure 11). To our knowledge, such one-way tunneling has never been reported.

Summary

We have investigated the isomerization of 1,4-dimethoxybenzene in low-temperature rare-gas matrixes by FTIR spectroscopy with the aid of the DFT/B3LYP/6-31++G**. From the results of the vibrational analysis and DFT calculations, the conformation of 1,4-dimethoxybenzene is found to be cis- and trans-planar. In argon matrixes, trans dissociates upon UV irradiation more rapidly than cis. The enthalpy difference between the more stable cis and the less stable trans is estimated from the dependence of the band intensities on the nozzle temperature, which is consistent with the value obtained by the DFT calculation. On the other hand, cis changes to trans in krypton and xenon matrixes. Especially, cis in the xenon matrixes is converted to trans completely. By assumption of the Arrhenius law, the effective activation energy from cis to trans is estimated to be 0.48 ± 0.13 kJ mol^{-1} from the rate constants determined below 30 K. It is concluded that the torsional potential surface of 1,4-dimethoxybenzene depends on the matrix media and the matrix temperature.

Acknowledgment. The authors thank Professor Kozo Kuchitsu (Faculty of Science, Josai University) and Professor Masao Takayanagi (Graduate School of BASE, Tokyo University of Agriculture and Technology) for their helpful discussion.

References and Notes

(1) Redington, R. L.; Redington, T. E. *J. Mol. Spectrosc.* **1979**, *78*, 229.

(2) Redington, R. L. *J. Chem. Phys.* **1990**, *92*, 6447.

(3) Redington, R. L.; Redington, T. E.; Montgomery, J. M. *J. Chem. Phys.* **2000**, *113*, 2304.

(4) Firth, D. W.; Barbara, P. F.; Trommsdorf, H. P. *Chem. Phys.* **1989**, *136*, 349.

(5) Rossetti, R.; Haddon, R. C.; Brus, L. E. *J. Am. Chem. Soc.* **1980**, *102*, 6913.

(6) Bondybey, V. E.; Haddon, R. C.; English, J. H. *J. Chem. Phys.* **1984**, *80*, 5432.

(7) Bondybey, V. E.; Haddon, R. C.; Rentzepis, P. M. *J. Am. Chem. Soc.* **1984**, *106*, 5969.

(8) Barbara, P. F.; Walsh, P. K.; Brus, L. E. *J. Phys. Chem.* **1989**, *93*, 29.

(9) Orendt, A. M.; Arnold, B. R.; Radziszewski, J. G.; Facelli, J. C.; Malsch, K. D.; Strub, H.; Grant, D. M.; Michl, J. *J. Am. Chem. Soc.* **1988**, *110*, 2648.

(10) Arnold, B. R.; Radziszewski, J. G.; Campion, A.; Perry, S. S.; Michl, J. *J. Am. Chem. Soc.* **1991**, *113*, 692.

(11) Frei, H.; Pimentel, G. C. *J. Phys. Chem.* **1981**, *85*, 3355.

(12) Hallou, A.; Schreiver-Mazzuoli, L.; Schriver, A.; Chaquin, P. *Chem. Phys.* **1998**, *237*, 251.

(13) Nieminen, J.; Murto, J.; J. Räsänen, J. *Spectrochim. Acta* **1991**, *47A*, 1495.

(14) Akai, N.; Kudoh, S.; Takayanagi, M.; Nakata, M. *Chem. Phys. Lett.* **2002**, *356*, 133.

(15) Akai, N.; Kudoh, S.; Takayanagi, M.; Nakata, M. *J. Phys. Chem. A* **2002**, *106*, 11029.

(16) Caminati, W.; Melandri, S.; Favero, L. B. *J. Chem. Phys.* **1994**, *100*, 8569.

(17) Anderson, G. M., III; Kollman, P. A.; Domelsmith, L. N.; Houk, K. N. *J. Am. Chem. Soc.* **1979**, *101*, 2344.

(18) Oikawa, A.; Abe, H.; Mikami, N.; Ito, M. *Chem. Phys. Lett.* **1985**, *116*, 463.

(19) Yamamoto, S.; Okuyama, K.; Mikami, N.; Ito, M. *Chem. Phys. Lett.* **1986**, *125*, 508.

(20) Breen, P. J.; Bernstein, E. R.; Secor, H. V.; Seeman, J. I. *J. Am. Chem. Soc.* **1989**, *111*, 1958.

(21) Tzeng, W. B.; Narayanan, K.; Hsieh, C. Y.; Tung, C. C. *J. Mol. Struct.* **1998**, *448*, 91.

(22) Patwari, G. N.; Doraiswamy, S.; Wategaonkar, S. *Chem. Phys. Lett.* **2000**, *316*, 433.

(23) Varsanyi, G. *Assignment of Vibrational Spectra of Seven Hundred Benzene Derivatives*; Wiley: New York, 1974.

(24) Nakata, M.; Kudoh, S.; Takayanagi, M.; Ishibashi, T.; Kato, C. *J. Phys. Chem.* **2000**, *104*, 11304.

(25) Kudoh, S.; Takayanagi, M.; Nakata, M. *J. Photochem. Photobiol. A* **1999**, *123*, 25.

(26) Frisch, M. J.; Trucks, G. W.; Schlegel, H. B.; Scuseria, G. E.; Robb, M. A.; Cheeseman, J. R.; Zakrzewski, V. G.; Montgomery, J. A.; Stratmann, R. E.; Burant, J. C.; Dapprich, S.; Millam, J. M.; Daniels, A. D.; Kudin, K. N.; Strain, M. C.; Farkas, O.; Tomasi, J.; Barone, V.; Cossi, M.; Cammi, R.; Mennucci, B.; Pomelli, C.; Adamo, C.; Clifford, S.; Ochterski, J.; Peterson, G. A.; Ayala, P. Y.; Cui, Q.; Morokuma, K.; Malick, D. K.; Rabuck, A. D.; Raghavachari, K.; Foresman, J. B.; Cioslowski, J.; Ortiz, J. V.; Stefanov, B. B.; Liu, G.; Liashenko, A.; Piskorz, P.; Komaromi, I.; Gomperts, R.; Martin, R. L.; Fox, D. J.; Keith, T.; Al-Laham, M. A.; Peng, C. Y.; Nanayakkara, A.; Gonzalez, C.; Challacombe, M.; Gill, P. M. W.; Johnson, B. G.; Chen, W.; Wang, M. W.; Andres, J. L.; Head-Gordon, M.; Replogle, E. S.; Pople, J. A. *Gaussian98*, Revision A.6; Gaussian, Inc.: Pittsburgh, PA, 1998.

(27) Becke, A. D. *J. Chem. Phys.* **1993**, *98*, 5648.

(28) Lee, C.; Yang, W.; Parr, R. G. *Phys. Rev. B* **1988**, *37*, 785.

(29) Akai, N.; Takayanagi, M.; Nakata, M. *Jpn. Chem. Program Exchange J.* **2001**, *13*, 97.

(30) Nagashima, N.; Kudoh, S.; Takayanagi, M.; Nakata, M. *J. Phys. Chem. A* **2001**, *105*, 10832.

(31) Hall, R. T.; Pimentel, G. C. *J. Chem. Phys.* **1963**, *38*, 1889.

(32) Knudsen, A. K.; Pimentel, G. C. *J. Chem. Phys.* **1983**, *78*, 6780.

(33) Kudoh, S.; Takayanagi, M.; Nakata, M.; Ishibashi, T.; Tasumi, M. *J. Mol. Struct.* **1999**, *479*, 41.

(34) Aspiala, A.; Lotta, T.; Murto, J.; Räsänen, M. *J. Chem. Phys.* **1983**, *79*, 4183.

(35) Räsänen, M.; Schwartz, G. P.; Bondybey, V. E. *J. Chem. Phys.* **1986**, *84*, 59.

(36) Squillacote, M. E.; Sheridan, R. S.; Chapman, O. L.; Anet, F. A. L. *J. Am. Chem. Soc.* **1979**, *101*, 3657.

(37) Kudoh, S.; Takayanagi, M.; Nakata, M. *Chem. Phys. Lett.* **1998**, *296*, 329.

(38) Ito, F.; Nakanaga, T.; Futami, Y.; Kudoh, S.; Takayanagi, M.; Nakata, M. *Chem. Phys. Lett.* **2001**, *343*, 185.

(39) Futami, Y.; Kudoh, S.; Takayanagi, M.; Nakata, M. *Chem. Phys. Lett.* **2002**, *357*, 209.

(40) Barnes, A. J. In Matrix Isolation Spectroscopy; Barnes, A. J., Orville-Thomas, W. J., Müller, A., Gaufrés, R., Eds.; Reidel: Dordrecht, 1981; p 531.

(41) Knözinger, E.; Babka E.; Hallamasek, D. *J. Phys. Chem. A* **2001**, *105*, 8176.